

## MAGNETIC-DIPOLAR-MODE OSCILLATIONS FOR NEAR- AND FAR-FIELD MANIPULATION OF MICROWAVE RADIATION

Eugene O. Kamenetskii\*, Roman Joffe, Maksim Berezin, Guy Vaisman, and Reuven Shavit

Microwave Magnetic Laboratory, Department of Electrical and Computer Engineering, Ben Gurion University of the Negev, Beer Sheva, Israel

**Abstract**—There has been a surge of interest in the subwavelength confinement effects of the electromagnetic fields. Based on these effects, one can obtain new behaviors of the near- and far-field radiation. It is well known that in optics, the subwavelength confinement can be obtained due to surface-plasmon (or electrostatic) oscillations in metal structures. This paper is a review of recent studies on the subwavelength confinement in microwaves due to magnetic-dipolar-mode (MDM) [or magnetostatic (MS)] oscillations in small ferrite samples. MDM oscillations in a mesoscopic ferrite-disk particle are quantized oscillations, which are characterized by energy eigenstates. The field structures are distinguished by power-flow vortices and non-zero helicity. Also in vacuum, the near fields originated from MDM particles are designated by topologically distinctive power-flow vortices, non-zero helicity, and a torsion degree of freedom. To differentiate such field structures from regular electromagnetic (EM) field structures, we term them as magnetoelectric (ME) fields. In a pattern of the microwave field scattered by a MDM ferrite disk and MDM-disk arrays, one can observe rotating topological-phase dislocations. This opens a perspective for creation of engineered electromagnetic fields with unique symmetry properties. In the near-field applications, we propose novel microwave sensors for material characterization, biology, and nanotechnology. Strong energy concentration and unique topological structures of the near fields originated from the MDM resonators allow effective measuring chiral properties of materials in microwaves. Generating

---

*Received 22 September 2013, Accepted 21 October 2013, Scheduled 24 October 2013*

\* Corresponding author: Eugene O. Kamenetskii (kmntsk@ee.bgu.ac.il).

Invited paper.

far-field orbital angular momenta from near-field microwave chirality of MDM structures can be a subject of a great interest. Realization of such vortex generators opens perspective for novel microwave systems with topological-phase modulation.

## 1. INTRODUCTION

In the search of novel communication systems, sensor devices and metamaterial structures, a strong interest arises in subwavelength particles as basic building blocks for controlling electromagnetic radiation. The effects of subwavelength confinement of the electromagnetic radiation allow engineering of novel field structures both in the near- and far-field regions. These effects concern fundamental problems of quasistatic oscillations in small objects: topological phases, vortex behaviors of the fields, the field chirality (helicity), and Fano-resonance interferences. Localization of electromagnetic energy in a subwavelength region presumes breaking the symmetry relationship between the time-varying electric and magnetic fields. Symmetry principles play an important role with respect to the laws of nature. Faraday's law gives evidence for existence of a magnetic displacement current. To put into symmetrical shape the equations coupling together the electric and magnetic fields, Maxwell introduced an electric displacement current. Such an additive, introduced for reasons of symmetry, resulted in appearing a unified field: the electromagnetic field. Dual symmetry between electric and magnetic fields underlies conservation of energy and momentum for electromagnetic fields [1]. It is well known, however, that in a general case of small (compared to the free-space electromagnetic-wave wavelength) samples made of media with strong temporal dispersion, the role of displacement currents in Maxwell equations can be negligibly small and the oscillating fields are quasistationary fields [2]. It is evident that when quasistatic oscillations in small objects occur, the electric-magnetic field symmetry is broken in Maxwell equations. What kinds of the time-varying fields can one expect to see when any (magnetic or electric) of the displacement currents is neglected?

Subwavelength confinement of light via electrostatic plasmonic resonances [3] has found more demand and has become an important issue in many research fields including integrated photonics, optical data storage, spectroscopy, microscopy, lithography, biological photonics, chemical studies, and so on (see, e.g., [4] and references therein). In optical plasmonics, different effects of the field symmetry breaking are used for subwavelength confinement of light. Recently, a novel concept for subwavelength optical power capture has been

developed. This concept is based on light recirculation through optical vortices: the vector fields of the time averaged optical powerflows in and around plasmonic nanostructures. The powerflow always occurs in the presence of the topological change. The phase singularities represent centers of local circulating optical power flows, or simply optical vortices [5]. On the other hand, it has been demonstrated that a helically grooved metal wire supports the propagation of chiral surface plasmon polaritons [6]. This offers the possibility to control both the chirality and the orbital angular momentum of electromagnetic fields at the subwavelength scale. Different plasmon chiral nanostructures draw promising routes for enhancing the optical near field, thus providing extended control over new functionalities in metamaterial science, biomimetics engineering and biosensing [6–9]. New results show unique possibilities for generating far-field optical vortex beams from near-field optical chirality [10]. Also, short-range interactions between discrete eigenstates of plasmon oscillations and the continuum of optical radiation, resulting in Fano resonances, is a subject of numerous modern investigations [11, 12].

In microwaves, however, the effects of subwavelength confinement due to quasistatic oscillations have not been studied sufficiently. Can one use the main ideas and results of the optical subwavelength plasmonics to create microwave structures with subwavelength confinement? Since resonance frequencies of electrostatic (plasmon) oscillations are very far from microwave frequencies, an answer to this question is negative. Nevertheless, there exists another type of subwavelength objects with quasistatic oscillations which show effective resonant interactions with microwave fields. There are small ferrite particles with magnetic-dipolar-mode (MDM) [or magnetostatic (MS)] oscillations [13]. In a series of recent publications, it was shown that small ferrite-disk particles may have unique spectral properties of MDM oscillations and the near fields originated from such particles are microwave superchiral fields with strong subwavelength localization of electromagnetic energy [14–21]. Specific long-distance topological properties of these fields are exhibited in the effects of path-dependent interference [22]. It was also shown that interaction of the MDM ferrite particle with its environment has a deep analogy with the Fano-resonance interference observed in natural and artificial atomic structures [23]. A ferrite is a magnetic dielectric with low losses. This may allow for electromagnetic waves to penetrate the ferrite and results in an effective interaction between the electromagnetic waves and magnetization within the ferrite. For MDM oscillations in a ferrite disk, magnetization dynamics is characterized by spin and orbital angular momentums and also by space and time symmetry breakings. This

presumes that the microwave fields near a ferrite disk should also have spin and orbital angular momentums and should be characterized by space and time symmetry breakings. To distinguish such fields from regular electromagnetic (EM) fields, we term them as magnetoelectric (ME) fields [20, 21].

The purpose of this paper is to review the effects of the near- and far-field microwave manipulation due to ferrite-disk particles with quasistatic MDM oscillations. We show that engineering of novel fields by these particles can open the perspective for unique microwave applications.

## 2. QUASISTATIC OSCILLATIONS IN SMALL SAMPLES

We start our studies with consideration of general aspects of quasistatic oscillations and a comparative analysis of two types of these oscillations: optical plasmonic (electrostatic) resonances in small metallic particles and microwave magnetic-dipolar (magnetostatic) resonances in small ferrite samples [20, 21]. In spite of the fact that subwavelength confinement of electromagnetic fields via electrostatic plasmonic resonances and magnetostatic magnon resonances have much common, there are evident fundamental differences between these oscillations. We will show why small particles with magnetostatic resonances can exhibit multiresonance oscillating spectra with ME properties (specific coupling between the time-varying electric and magnetic fields in a subwavelength region) and no such properties can be observed in a case of small particles with electrostatic resonances.

For a case of plasmonic (electrostatic) resonances in small metallic samples, one neglects a magnetic displacement current and has quasistationary electric fields. A dual situation is demonstrated for magnetic-dipolar (magnetostatic) resonances in small ferrite samples, where one neglects an electric displacement current. As an appropriate approach for description of quasistatic oscillations in small particles, one uses a classical formalism where the material linear response at frequency  $\omega$  can be described by a local bulk dielectric function — the permittivity tensor  $\vec{\epsilon}(\omega)$  — or by a local bulk magnetic function — the permeability tensor  $\vec{\mu}(\omega)$ . With such an approach (and in neglect of a corresponding displacement current) one can introduce a notion of a scalar potential: an electrostatic potential  $\varphi$  for electrostatic oscillations and a magnetostatic potential  $\psi$  for magnetostatic resonances. It is evident that these potentials do not have the same physical meaning as in the problems of “pure” (non-time-varying) electrostatic and magnetostatic fields [1, 2]. Because of the resonant behaviors of small dielectric/metallic or small

magnetic objects [confinement phenomena plus temporal-dispersion conditions of tensors  $\vec{\varepsilon}(\omega)$  or  $\vec{\mu}(\omega)$ ], one has scalar *wave* functions: an electrostatic-potential wave function  $\phi(\vec{r}, t)$  and a magnetostatic-potential wave function  $\psi(\vec{r}, t)$ , respectively. The main note is that since we are on a level of the continuum description of media [based on tensors  $\vec{\varepsilon}(\omega)$  or  $\vec{\mu}(\omega)$ ], the boundary conditions for quasistatic oscillations should be imposed on scalar wave functions  $\phi(\vec{r}, t)$  or  $\psi(\vec{r}, t)$  and their derivatives, but not on the RF functions of polarization (plasmons) or magnetization (magnons). One has to keep in mind that in phenomenological models based on the effective-medium [the  $\vec{\varepsilon}(\omega)$ - or  $\vec{\mu}(\omega)$ -continuum] description, no electron-motion equations and boundary conditions corresponding to these equations are used.

Fundamentally, subwavelength sizes should eliminate any effects of the electromagnetic retardation. When one neglects the displacement currents (magnetic or electric) and considers scalar functions  $\phi(\vec{r}, t)$  or  $\psi(\vec{r}, t)$  as the wave functions, one becomes faced with important questions, whether there could be the *propagation behaviors* inherent for the quasistatic wave processes and, if any, what is the nature of these retardation effects. In a case of electrostatic resonances, the Ampere-Maxwell law gives the presence of a curl magnetic field. With this magnetic field, however, one cannot define the power-flow density of propagating electrostatic-resonance waves. Certainly, from a classical electrodynamics point of view [1], one does not have a physical mechanism describing the effects of transformation of a curl magnetic field to a potential electric field. In like manner, one can see that in a case of magnetostatic resonances, the Faraday law gives the presence of a curl electric field. With this electric field one cannot define the power-flow density of propagating magnetostatic-resonance waves since, from a classical electrodynamics point of view, one does not have a physical mechanism describing the effects of transformation of a curl electric field to a potential magnetic field [1]. So, from Maxwell equations it follows that in a case of electrostatic resonances, characterizing by a scalar wave function  $\phi(\vec{r}, t)$ , the time-varying electric fields cannot be accompanied at all with the RF magnetic fields and, similarly, in a case of magnetostatic resonances, characterizing by scalar wave function  $\psi(\vec{r}, t)$ , the time-varying magnetic fields cannot be accompanied at all with the RF electric field. This fact is perceived, in particular, from the following remarks by McDonald [24, 25]. In frames of the quasiolestatic approximation, we introduce electrostatic-potential function  $\phi(\vec{r}, t)$  excluding completely the magnetic displacement current:  $\frac{\partial \vec{B}}{\partial t} = 0$ . At the same time, from the Maxwell equation (the Ampere-Maxwell law),  $\nabla \times \vec{H} = \frac{1}{c} \frac{\partial \vec{D}}{\partial t}$ , we write that  $\nabla \times$

$\frac{\partial \vec{H}}{\partial t} = \frac{1}{c} \frac{\partial^2 \vec{D}}{\partial t^2}$ . If a sample does not possess any magnetic anisotropy, we have  $\frac{\partial^2 \vec{D}}{\partial t^2} = 0$ . Similarly, in frames of the quasimagnetostatic approximation, we introduce magnetostatic-potential function  $\psi(\vec{r}, t)$  excluding completely the electric displacement current:  $\frac{\partial \vec{D}}{\partial t} = 0$ . From Maxwell equation (the Faraday law),  $\nabla \times \vec{E} = -\frac{1}{c} \frac{\partial \vec{B}}{\partial t}$ , we obtain that  $\nabla \times \frac{\partial \vec{E}}{\partial t} = -\frac{1}{c} \frac{\partial^2 \vec{B}}{\partial t^2}$ . If a sample does not possess any dielectric anisotropy, we have  $\frac{\partial^2 \vec{B}}{\partial t^2} = 0$ . From the above equations on the second derivatives of the fields ( $\frac{\partial^2 \vec{D}}{\partial t^2} = 0$  and  $\frac{\partial^2 \vec{B}}{\partial t^2} = 0$ ), it follows that the electric field in small resonant dielectric/metallic objects as well as the magnetic field in small resonant magnetic objects vary linearly with time. This leads, however, to arbitrary large fields at early and late times, and is excluded on physical grounds. An evident conclusion suggests itself at once: the electric field (for electrostatic resonances) and the magnetic field (for magnetostatic resonances) are constant quantities. Such a conclusion contradicts the fact of temporally dispersive media and thus any resonant conditions. Another conclusion is more unexpected: the Ampere-Maxwell law is not valid for electrostatic resonances and the Faraday law is not valid for magnetostatic resonances. The above analysis definitely means that, from classical electrodynamics, the spectral problem formulated *exceptionally* for the electrostatic-potential wave function  $\phi(\vec{r}, t)$  do not presume use of alternative magnetic fields and, similarly, the spectral problem formulated *exceptionally* for the magnetostatic-potential function wave  $\psi(\vec{r}, t)$  do not presume use of alternative electric fields. This statement lives open a question on the existence of propagation-wave behaviors for the quasistatic-resonance processes.

The eigenvalue problem for electrostatic resonances in nanoparticles occurs at optical frequencies when an isotropic dielectric medium exhibits strong temporal dispersion and its real part assumes a negative value. The resonant wavelengths are determined by shapes of nanostructures and dielectric responses of constituents [26, 27]. When the material linear response is described by a bulk dielectric scalar function  $\varepsilon(\omega)$ , the electrostatic resonances can be found as solutions of the equation [28]:

$$\vec{\nabla} \cdot \left( \varepsilon(\vec{r}) \vec{\nabla} \phi \right) = 0. \quad (1)$$

For homogeneous negative permittivity particles ( $\varepsilon_p < 0$ ) in a uniform transparent immersion medium ( $\varepsilon_s > 0$ ) and with use of conventional Dirichlet-Neumann boundary conditions for electrostatic-potential function, this equation acquires a form of a linear generalized

eigenvalue problem:

$$\vec{\nabla} \cdot \left( \theta(\vec{r}) \vec{\nabla} \phi \right) = s \nabla^2 \phi, \quad (2)$$

where  $\theta(\vec{r})$  equals 1 inside the particle and zero outside the particle, and  $s = 1/(1 - \varepsilon_p/\varepsilon_s)$ . The eigenmodes (surface plasmons) are orthogonal and are assumed to be normalized as [28, 29]

$$\int \phi_q^*(\vec{r}) \nabla^2 \phi_{q'}(\vec{r}) d^3r = \delta_{q,q'}. \quad (3)$$

It was pointed out that for electrostatic resonances in nanoparticles one has a non-Hermitian eigenvalue problem with bi-orthogonal (instead of regular-orthogonal) eigenfunctions [30]. Electrostatic (plasmonic) resonance excitations, existing for particle sizes much smaller than the free-space electromagnetic wavelength, are described by the *evanescent-wave* electrostatic-potential functions  $\phi(\vec{r}, t)$ . No retardation effects are presumed in such a description. In optics, the above electrostatic theory applies only to nanoparticles, when electromagnetic retardation effects are negligible. For a spherical nanoparticle of arbitrary radius provided that the latter is much smaller than the free-space wavelength of incident optical radiation, the resonance permittivity values are consistent with the classical Mie theory [31]. In an analysis of scattered electromagnetic fields, a small metal particle with electrostatic oscillations can be treated as a point electric dipole precisely oriented in space [32, 33]. Importantly, a role of the magnetic field in plasmonic oscillations becomes appreciable only when one deviates from the electrostatic approximation to the full-Maxwell-equation description. So the retardation effects appear when particle sizes are comparable with the free-space electromagnetic wavelength. Corrections to electrostatic resonance modes due to retardation can be found by using series expansions of the solutions to time harmonic Maxwell equations with respect to the small ratio of the object size to the free-space wavelength. There is the electromagnetic-wave process with a coupling between the electric and magnetic fields [34]. It was shown recently that anomalous light scattering with quite unusual scattering diagrams and enhanced scattering cross sections near plasmon (polariton) resonance frequencies is non-Rayleigh scattering. The observed power-flow patterns cannot be understood within the frame of a dipole approximation and the terms of higher orders with respect to size parameter  $q = 2\pi a/\lambda$  should be taken into account [35–37].

At microwave frequencies, the eigenvalue problem for magneto-static resonances in small ferrite particles is quite different. The spectral properties of these resonances are analyzed based on the Walker

equation for MS-potential wave function  $\psi(\vec{r}, t)$  [38]:

$$\vec{\nabla} \cdot (\vec{\mu} \cdot \vec{\nabla} \psi) = 0 \quad (4)$$

Outside a ferrite this equation becomes the Laplace equation. A distinctive feature of MDM resonances in small ferrite samples with certain geometrical forms is the fact that because of the bias-field induced anisotropy in a ferrite, one may obtain the *real-eigenvalue spectra* for scalar wave functions. In microwave experiments with quasi-2D ferrite disks, regular multiresonance MDM spectra have been observed [39–43]. A formulation of quasi-Hermitian eigenvalue problem and analytical spectral solutions for MDMs in these thin-film ferrite disks were shown recently [14–17]. Solutions are *propagating-wave* scalar functions  $\psi(\vec{r}, t)$ . This presumes *non-electromagnetic* (magnetostatic) retardation effects in such small ferrite samples. In solving a spectral problem for MDM oscillations, special aspects concern properties of the RF electric fields. It is very important that a role of the electric fields in MDM ferrite particles becomes evident when one does not deviate from the MS description to the full-Maxwell-equation description. These electric fields appear due to magnetic currents with topological-phase nature. Because of dynamics of the magnetization motion in a ferrite disk, characterizing by symmetry breakings, small ferrite particles with MDM spectra originate near fields with unique topological properties. We term these fields as magnetoelectric (ME) fields [20, 21]. The ME fields are characterized by helical structures and power-flow vortices. Scattering of the EM fields from the MDM-vortex particles is purely topological. For incident EM waves, the vortex topological singularities act as traps, providing strong subwavelength confinement of the microwave fields [17, 18]. It appears that a vortex may turn out to generate a “radius of no return”, beyond which the incident EM fields falls inevitably towards the vortex singularity. In such a case, the MDM vortex becomes an EM “black hole” in microwaves [18–22].

We should come back now to the McDonald’s statement [24, 25] that, from a formal point of view, no RF magnetic fields are available in a case of electrostatic resonances and no RF electric fields are available in a case of magnetostatic resonances. As we discussed in this section, in particles with plasmonic oscillations one has a non-Hermitian eigenvalue problem and the retardation effects appear when particle sizes are comparable with the free-space electromagnetic wavelength. So a role of the magnetic field in plasmonic oscillations becomes appreciable only when one deviates from the electrostatic approximation to the full-Maxwell-equation description. In a case of MDM resonances in small ferrite particles, situation is completely

different. In these particles one has specific magnetostatic-wave retardation effects. The electric fields arising from the MDM spectral solutions are characterized by topological properties. This results in appearance of peculiar fields — the ME fields. The helicity parameters of ME fields give evidence for violation of Faraday law and, consequently, violation of Lorentz invariance [20–23].

### 3. ENERGY EIGENSTATES OF MDM OSCILLATIONS IN A QUASI-2D FERRITE DISK

MDM oscillations in a quasi-2D ferrite disk are macroscopically quantized states. Long range dipole-dipole correlation in position of electron spins in a ferromagnetic sample can be treated in terms of collective excitations of the system as a whole. If the sample is sufficiently small so that the dephasing length  $L_{ph}$  of the magnetic dipole-dipole interaction exceeds the sample size, this interaction is non-local on the scale of  $L_{ph}$ . This is a feature of mesoscopic ferrite samples, i.e., samples with linear dimensions smaller than  $L_{ph}$  but still much larger than the exchange-interaction scales.

In a case of a quasi-2D ferrite disk, the quantized forms of these collective matter oscillations — magnetostatic magnons — were found to be quasiparticles with both wave-like and particle-like behavior, as expected for quantum excitations. The magnon motion in this system is quantized in the direction perpendicular to the plane of a ferrite disk. The MDM oscillations in a ferrite disk, analyzed as spectral solutions for the MS-potential wave function  $\psi(\vec{r}, t)$ , has evident quantum-like attributes [14–17, 20, 21]. For disk geometry, the energy-eigenstate oscillations are described by a two-dimensional (with respect to in-plane coordinates of a disk) differential operator  $\hat{G}$ :

$$\hat{G}_{\perp} = \frac{g_q}{16\pi} \mu \nabla_{\perp}^2, \quad (5)$$

where  $\nabla_{\perp}^2$  is the two-dimensional Laplace operator,  $\mu$  is a diagonal component of the permeability tensor, and  $g_q$  is a dimensional normalization coefficient for mode  $q$ . Operator  $\hat{G}_{\perp}$  is positive definite for negative quantities  $\mu$ . The normalized average (on the RF period) density of accumulated magnetic energy of mode  $q$  is determined as

$$E_q = \frac{g_q}{16\pi} (\beta_{z_q})^2, \quad (6)$$

where  $\beta_{z_q}$  is the propagation constant of mode  $q$  along the disk axis  $z$ . The energy eigenvalue problem is defined by the differential equation:

$$\hat{G}_{\perp} \tilde{\eta}_q = E_q \tilde{\eta}_q, \quad (7)$$

where  $\tilde{\eta}_q$  is a dimensionless membrane (“in-plane”) MS-potential wave function. At a constant frequency, the energy orthonormality for MDMs in a ferrite disk is written as:

$$(E_q - E_{q'}) \int_S \tilde{\eta}_q \tilde{\eta}_{q'}^* dS = 0, \quad (8)$$

where  $S$  is a cylindrical cross section of a ferrite disk. One has different mode energies at different quantities of a bias magnetic field. From the principle of superposition of states, it follows that wave functions  $\tilde{\eta}_q$  ( $q = 1, 2, \dots$ ), describing our quantum system, are vectors in an abstract space of an infinite number of dimensions — the Hilbert space. In quantum mechanics, this is the case of so-called energetic representation, when the system energy runs through a discrete sequence of values. In the energetic representation, a square of a modulus of the wave function defines probability to find a system with a certain energy value. In our case, scalar-wave membrane function  $\tilde{\eta}$  can be represented as

$$\tilde{\eta} = \sum_q a_q \tilde{\eta}_q \quad (9)$$

and the probability to find a system in a certain state  $q$  is defined as

$$|a_q|^2 = \left| \int_S \tilde{\eta} \tilde{\eta}_q^* dS \right|^2. \quad (10)$$

The statement that confinement phenomena for MS oscillations in a normally magnetized ferrite disk demonstrate typical atomic-like properties of discrete energy levels can be well illustrated by an analysis of the experimental absorption spectra in Refs. [39, 40] obtained at a varying bias magnetic field and a constant operating frequency. The main feature of the multi-resonance line spectra in Refs. [39, 40] is the fact that high-order peaks correspond to lower quantities of the bias magnetic field. Physically, the situation looks as follows. Let  $H_0^{(A)}$  and  $H_0^{(B)}$  be, respectively, the upper and lower values of a bias magnetic field corresponding to the borders of a spectral region. We can estimate a total depth of a “potential well” as:  $\Delta U_{AB} = -4\pi \int M_0 (H_0^{(A)} - H_0^{(B)}) dV$ , where  $M_0$  is the saturation magnetization. Let  $H_0^{(1)}$  be a bias magnetic field, corresponding to the main absorption peak in the experimental spectrum ( $H_0^{(B)} < H_0^{(1)} < H_0^{(A)}$ ). When we put a ferrite sample into this field, we supply it with the energy:  $-4\pi \int M_0 H_0^{(1)} dV$ . To some extent, this is a pumping-up energy. Starting from this level, we can excite the entire spectrum from the

main mode to the high-order modes. As a value of a bias magnetic field decreases, the particle obtains higher levels of negative energy. One can estimate the negative energies necessary for transitions from the main level to upper levels. For example, to have a transition from the first level  $H_0^{(1)}$  to the second level  $H_0^{(2)}$  ( $H_0^{(B)} < H_0^{(2)} < H_0^{(1)} < H_0^{(A)}$ ) we need the energy surplus:  $\Delta U_{12} = -4\pi \int M_0(H_0^{(1)} - H_0^{(2)})dV$ . The situation is very resembling the increasing a negative energy of the hole in semiconductors when it “moves” from the top of a valence band. In a classical theory, negative-energy solutions are rejected because they cannot be reached by a continuous loss of energy. But in quantum theory, a system can jump from one energy level to a discretely lower one; so the negative-energy solutions cannot be rejected, out of hand. When, for given frequency  $\omega$ , one continuously varies the quantity of the DC field  $H_0$ , one sees a discrete set of absorption peaks. It means that one has the discrete-set levels of potential energy. The line spectra appear due to the quantum-like transitions between energy levels of a ferrite disk particle. As a quantitative characteristic of permitted quantum transitions, there is the probability, which define the intensities of spectral lines. The discrete nature of the MS-magnon states requires a minimum of energy to excite a MS magnon, which is equivalent to having an energy gap. There are energy gap scales with the bias magnetic field at a given operating frequency. In paper [44], it was shown that because of the discrete energy eigenstates of MDM oscillations resulting from structural confinement in a ferrite disk, one can describe the oscillating system as collective motion of quasiparticles — the “light magnons”.

From Equations (5)–(7) it follows that MDM resonances in a ferrite disk correspond to discrete quantities of the permeability-tensor component  $\mu$ . This component is defined as [13]

$$\mu = 1 + \frac{\gamma^2 M_0 H_0}{\gamma^2 H_0^2 - \omega^2}, \quad (11)$$

where  $\gamma$  is the gyromagnetic ratio. It is evident that discrete energy eigenstates of MDM oscillations can be obtained also by variation of operating frequency at a constant bias magnetic field. So, for given disk sizes and a given quantity of saturation magnetization  $M_0$ , there are two different mechanisms of energy quantization: (i) quantization by a bias field  $H_0$  at a constant signal frequency  $\omega$  and (ii) quantization by signal frequency  $\omega$  at a constant bias field  $H_0$ . Let us consider a certain frequency  $f'$ . For observation of energy quantization levels at this frequency, there exists a specific set of the bias-field quantities:  $(H_0^{(1)})'$ ,  $(H_0^{(2)})'$ ,  $(H_0^{(3)})'$ , ... On the other hand, for a given bias magnetic field, there is a specific set of the frequency quantization

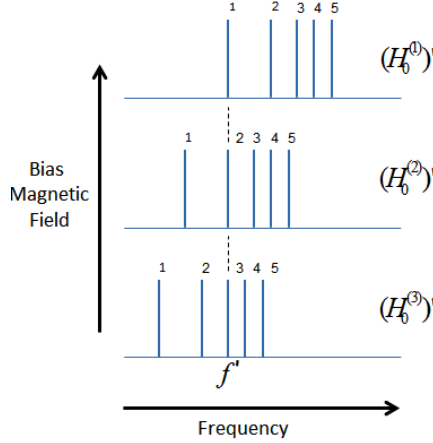


**Figure 1.** Correlation between two mechanisms of energy quantization: Quantization by signal frequency and quantization by a bias magnetic field.

levels. Figure 1 illustrates correlation between the two mechanisms of energy quantization. It becomes evident that there should be a certain uncertainty limit stating that

$$\Delta f \Delta H_0 \geq \text{uncertainty limit.} \quad (12)$$

The uncertainty limit is a constant which depends on the disk size parameters and ferrite material properties. It is evident that beyond the frames of the uncertainty limit (12), one has continuum of energy. The fact that there are different mechanisms of energy quantization gives us possibility to conclude that for MDM oscillations in a quasi-2D ferrite disk one can have discrete energy eigenstates as well as continuum of energy. It is worth noting that, in general, for different types of subwavelength particles, the uncertainty principle may acquire different forms. An interesting variant of Heisenberg's uncertainty principle was shown recently in subwavelength optics [3]. Applied to the optical field, this principle says that we can only measure the electric or the magnetic field with accuracy when the volume in which they are contained is significantly smaller than the wavelength of light in all three spatial dimensions. As volumes smaller than the wavelength are probed, measurements of optical energy become uncertain, highlighting the difficulty with performing measurements in this regime.

The above analysis of energy eigenstates gives possibility for deeper understanding of the nature of the experimentally observed

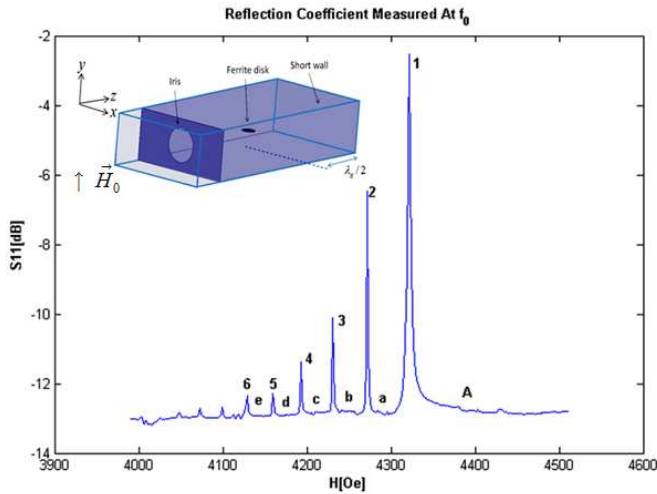


**Figure 2.** An experimental multiresonance spectrum of modulus of the reflection coefficient obtained by varying a bias magnetic field and at a resonant frequency of  $f_0 = 7.4731$  GHz. The resonance modes are designated in succession by numbers  $n = 1, 2, 3, \dots$ . The states beyond resonances are designated with small letters  $a, b, c, \dots$ . An insert shows a  $TE_{102}$ -mode rectangular waveguide cavity with a normally magnetized ferrite-disk sample. Figure reproduced from Ref. [23].

multiresonance spectra of microwave oscillations in a microwave cavity originated from a MDM ferrite disk [23, 39–43]. These spectra were obtained by varying a bias magnetic field at a constant operating frequency, which is a resonant frequency of the cavity. An example of such a spectrum, studied in Ref. [23], is shown in Figure 2. The resonance modes are designated in succession by numbers  $n = 1, 2, 3, \dots$ , while the states beyond resonances are designated with small letters  $a, b, c, \dots$ . This spectrum is obtained for a normally magnetized ferrite-disk sample placed in a rectangular waveguide cavity with the  $TE_{102}$  resonant mode. A resonant frequency is  $f_0 = 7.4731$  GHz. The disk axis is oriented along the waveguide  $E$ -field and the disk position is in a maximum of the RF magnetic field of the cavity (see an insert in Figure 2). In Ref. [23], we used a disk sample of diameter  $2R = 3$  mm made of the yttrium iron garnet (YIG) film on the gadolinium gallium garnet (GGG) substrate (the YIG film thickness  $d = 49.6$   $\mu\text{m}$ , saturation magnetization  $4\pi M_0 = 1880$  G, linewidth  $\Delta H = 0.8$  Oe; the GGG substrate thickness is 0.5 mm).

Figures 3 and 4 give explanations why this multiresonance

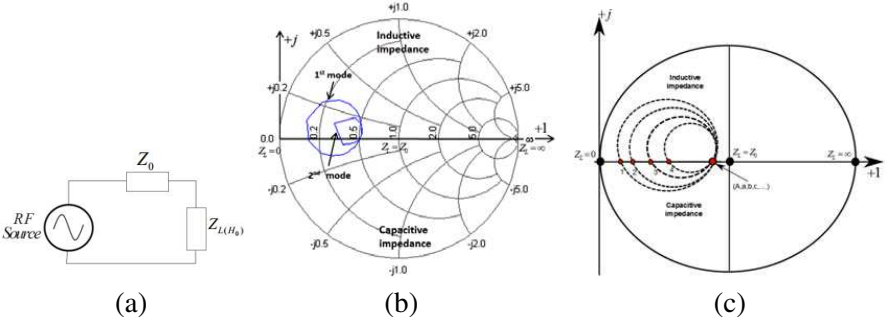


**Figure 3.** Quantized variations of an input impedance of a cavity at MDM resonances. (a) An equivalent electric circuit of an experimental setup. (b) Experimental results of the quantized-state impedances for modes 1 and 2 plotted on the complex-reflection-coefficient plane. (c) The entire-spectrum impedances shown schematically as a set of circles on the complex-reflection-coefficient plane. Red dots show quantized states with pure active quantities of the cavity impedance. Figures (a), (b), and (c) reproduced from Ref. [23].

spectrum of microwave oscillations can be related to the energy eigenstates of MDMs in a ferrite disk. Figure 3(a) shows an equivalent electric circuit of an experimental setup: a source with internal impedance  $Z_0$  supplies a cavity with an embedded ferrite disk by microwave energy of frequency  $f_0$ ; a load impedance,  $Z_L$ , — an input impedance of a cavity — is varied by an external parameter — a bias magnetic field  $H_0$ . Due to MDM resonances in a ferrite particle, the cavity impedances become quantized states. This can be well illustrated by a Smith chart — a complex-plane nomogram designed for graphical display of impedance multiple parameters [45]. Figure 3(b) shows experimental results of the quantized-state impedances for modes 1 and 2 plotted on the complex-reflection-coefficient plane. The entire-spectrum impedances are shown schematically in Figure 3(c) as a set of circles on the complex-reflection-coefficient plane. Red dots correspond to quantized states with pure active quantities of the cavity impedance. Since we have a constant resonant frequency, the shown resonances are not the modes due to quantization of the photon wave vector in a cavity. So the question arises: What is the nature of the modes observed in a cavity at a constant frequency? It is evident that the discrete variation of the cavity impedances and so the discrete states of the cavity fields are caused by the discrete variation of energy of a ferrite disk, appearing due to an external source of

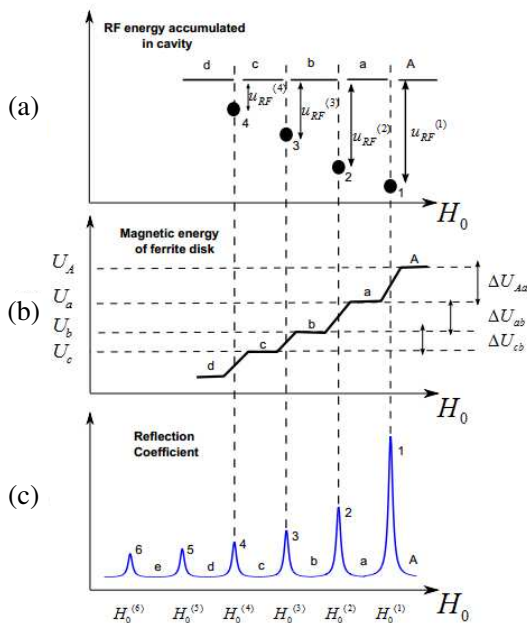


**Figure 4.** Quantized states of RF energy in a cavity and magnetic energy in a disk. (a) RF energy accumulated in a cavity. (b) Magnetic energy of a ferrite disk. (c) Multiresonance spectrum of modulus of the reflection coefficient. Figures (a), (b), and (c) reproduced from Ref. [23].

energy — a bias magnetic field. Suppose that we have our microwave system at a quantity of a bias magnetic field above the 1st peak in the resonance spectrum. In Figure 2, this state is designated by a capital letter  $A$ . The corresponding bias magnetic field, designated as  $H_0^{(A)}$ , supplies a ferrite disk by energy:  $U_A = -4\pi \int M_0 H_0^{(A)} dV$ . At this bias magnetic field, a cavity (with an embedded ferrite disk) has good impedance matching and can accumulate certain microwave energy. When we consider the state  $a$  (the state beyond resonances 1 and 2), a cavity has the same good impedance matching and the same level of accumulated microwave energy. But the energy supplied to a ferrite disk by a bias magnetic field is reduced by a quantity  $U_A - U_a \equiv \Delta U_{Aa} = -4\pi \int M_0 (H_0^{(A)} - H_0^{(a)}) dV$ . At a very narrow region of a bias magnetic field corresponding to the 1st resonance-peak position,  $H_0^{(1)}$ , RF energy accumulated in the cavity is strongly reduced because of increasing of the active-quantity cavity impedance

[see Figure 3(c)]. This reduction of the RF energy (designated as  $u_{\text{RF}}^{(1)}$ ) must be equal in magnitude to quantity  $\Delta U_{Aa}$ . Such kind of relationship between magnetic energy of a disk and RF energy of a cavity is exhibited also for other peaks in a spectrum. For the entire spectrum, in Figure 4 we give qualitative pictures of potential energy of a ferrite disk and discrete states of the RF energy accumulated in the cavity with respect to a bias magnetic field. These states are shown in correlation with the spectral picture for the reflection coefficient. From peak to peak one has discrete-portion reduction of the disk magnetic energy. Due to such a discrete-portion reduction of the disk magnetic energy we observe excitation of the RF resonance peaks.

#### 4. INTERACTION OF MDMs WITH THE ENVIRONMENTAL MICROWAVE RADIATION

When the above analysis explains why the experimentally observed multiresonance spectrum of microwave oscillations can be related to the energy eigenstates of MDMs in a ferrite disk, the question how the MDMs interact with the environmental microwave radiation remains open. Analytically, there are two spectral models for the MDM oscillations in a ferrite disk. These models are based on so-called the  $G$ - and  $L$ -mode spectral solutions [14–22]. The  $G$ -modes, are associated with a considered above differential operator  $G$ . There are modes with Hermitian Hamiltonian for MS-potential wave functions  $\psi(\vec{r}, t)$ . The  $G$ -modes are related to the discrete energy states of MDMs. In a case of the  $L$ -modes, one has a complex Hamiltonian for MS-potential wave functions  $\psi(\vec{r}, t)$ . For eigenfunctions associated with such a complex Hamiltonian, we have nonzero Berry potential (meaning the presence of geometric phases). The main difference between the  $G$ - and  $L$ -mode solutions becomes evident when one considers the boundary conditions on a lateral surface of a ferrite disk. In solving the energy-eigenstate spectral problem for the  $G$ -mode states, the boundary condition on a lateral surface of a ferrite disk, are expressed as

$$\mu \left( \frac{\partial \tilde{\eta}}{\partial r} \right)_{r=\mathfrak{R}^-} - \left( \frac{\partial \tilde{\eta}}{\partial r} \right)_{r=\mathfrak{R}^+} = 0, \quad (13)$$

where  $\tilde{\eta}$  is the MS-potential membrane wave function (for the  $G$ -mode solution) and  $\mathfrak{R}$  a radius of a ferrite disk. There is a homogeneous boundary condition for a differential operator  $\hat{G}_\perp$  [see Equation (5)]. This boundary condition, however, manifests itself in contradictions with the electromagnetic boundary condition for a radial component of magnetic flux density  $\vec{B}$  on a lateral surface of a ferrite-disk resonator.

Such a boundary condition, used in solving the resonant spectral problem for the  $L$ -mode states, is written as

$$\mu(H_r)_{r=\Re^-} - (H_r)_{r=\Re^+} = -i\mu_a(H_\theta)_{r=\Re}, \quad (14)$$

where  $(H_r)_{r=\Re^-}$  and  $(H_r)_{r=\Re^+}$  are radial components of a magnetic field on a border circle, and  $(H_\theta)_{r=\Re}$  is an azimuth magnetic field on a border circle. In the magnetostatic description, this equation appears as

$$\mu \left( \frac{\partial \tilde{\varphi}}{\partial r} \right)_{r=\Re^-} - \left( \frac{\partial \tilde{\varphi}}{\partial r} \right)_{r=\Re^+} = -\mu_a \nu (\tilde{\varphi})_{r=\Re^-}, \quad (15)$$

where  $\tilde{\varphi}$  is the MS-potential membrane wave function (for the  $L$ -mode solution),  $\nu$  an azimuth wave number, and  $\mu_a$  an off-diagonal component of the permeability tensor. The spectral-problem solutions based on Equation (13) are single-valued-function solutions. At the same time, the spectral-problem solutions based on Equation (15) are nonsingle-valued-function solutions. Because of dependence of the right-hand side of Equation (15) on a sign of the azimuth wave number, the two (clock and counterclockwise) types of resonant solutions may exist at a given direction of a bias magnetic field. In the microwave measurement, we do not distinguish such clockwise and counterclockwise types of MDM oscillations. The signals measured at the ports of a microwave system are single-valued functions. It was shown [19] that to get real-quantity eigenstates of the  $L$ -mode solutions, a special differential operator acting on the boundary conditions on a lateral surface of a ferrite disk should be introduced. As the eigenstates of this operator, there are topological-phase circular magnetic currents. These magnetic currents result in appearance of fluxes of gauge electric fields [16, 17, 19–21].

The electric and magnetic fields originated from the  $L$ -mode spectral solutions are the states with specific spin and orbital rotational motion of the field vectors. These fields, characterizing by eigen power-flow vortices and helicity parameters, are called magnetoelectric (ME) fields [20, 21]. The ME field solutions (which can be obtained by numerical integration with the HFSS-program simulation) give evidence for spontaneous symmetry breakings of the resonant states. Because of rotations of localized field configurations in a fixed observer inertial frame, coupling between EM and ME fields cause violation of the Lorentz symmetry of spacetime. In such a sense, ME fields can be considered as Lorentz-violating extension of the Maxwell equations. To characterize the ME-field singularities, the helicity parameter was introduced. The helicity parameter for the near fields of a ferrite disk with MDM oscillations is defined as [20, 21]

$$F = \frac{\epsilon_0}{4} \text{Im} \left\{ \vec{E} \cdot \left( \vec{\nabla} \times \vec{E} \right)^* \right\}. \quad (16)$$

We can also introduce a normalized helicity parameter, which shows a time-averaged space angle between rotating vectors  $\vec{E}$  and  $\vec{\nabla} \times \vec{E}$ :

$$\cos \alpha = \frac{\text{Im} \left\{ \vec{E} \cdot \left( \vec{\nabla} \times \vec{E} \right)^* \right\}}{\left| \vec{E} \right| \left| \nabla \times \vec{E} \right|}, \quad (17)$$

In the regions where this parameter is not equal to zero, a space angle between the vectors  $\vec{E}$  and  $\vec{\nabla} \times \vec{E}$  is not equal to  $90^\circ$ . This breaks the field structure of Maxwell electrodynamics.

One becomes evident with the fact that due to properties of MDM oscillations, the fields of a microwave structure with an embedded ferrite disk are characterized not only by discrete energy levels, but also by specific topological eigenstates. This gives possibility for unique manipulation of microwave radiation.

## 5. MANIPULATING MICROWAVES WITH MDM FERRITE PARTICLES

MDM oscillations in a quasi-2D ferrite disk show dynamical symmetry properties resulting in appearance of topologically distinct structures of the fields. For the first time, the rotating field configurations and power-flow vortices inside a ferrite disk were shown for the  $L$ -mode

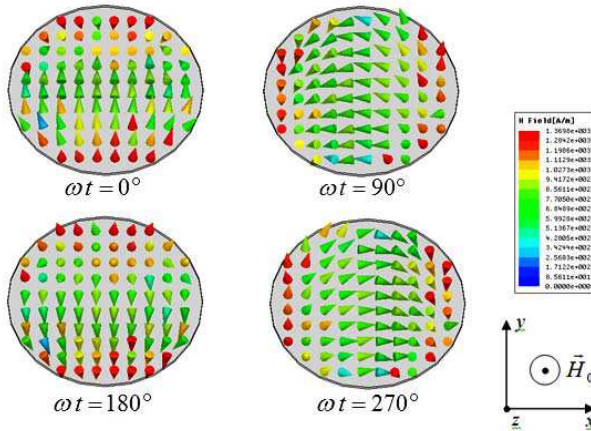


**Figure 5.** A perspective view for the numerically modeled magnetic field distributions on the upper plane of a ferrite disk for the for the 1st resonance state ( $f = 8.52$  GHz) at different time phases. Figure reproduced from Ref. [46] @2009 IOP Publ. and Ref. [47] @2009 AIP.

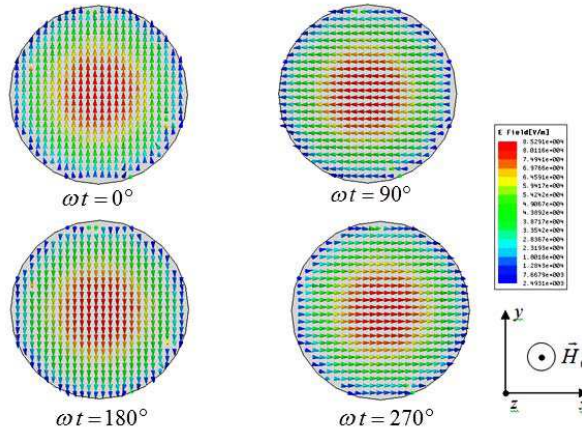


**Figure 6.** A top view for the numerically modeled electric field distributions on the upper plane of a ferrite disk for the for the 1st resonance state ( $f = 8.52$  GHz) at different time phases. Figure reproduced from Ref. [46] @2009 IOP Publ. and Ref. [47] @2009 AIP.

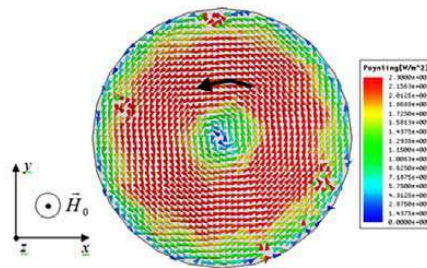


**Figure 7.** The power flow density distribution for the 1st mode ( $f = 8.52$  GHz) in a quasi-2D ferrite disk. Figure reproduced from Ref. [46] @2009 IOP Publ.

spectra in Refs. [46, 47]. Figures 5 and 6 show a typical configuration of rotating electrical and magnetic fields inside a ferrite disk for the 1st MDM. This field configuration results in appearance of a power-flow-density vortex (see Figure 7). Similar configurations of rotating fields and a power-flow-density vortex for the 2nd MDM are shown in Figures 8–10. In the vicinity of a ferrite disk with a MDM resonance, one has a power-flow whirlpool. For an incident EM wave, such a vortex topological singularity acts as a trap, providing strong subwavelength confinement and symmetry breakings of the microwave

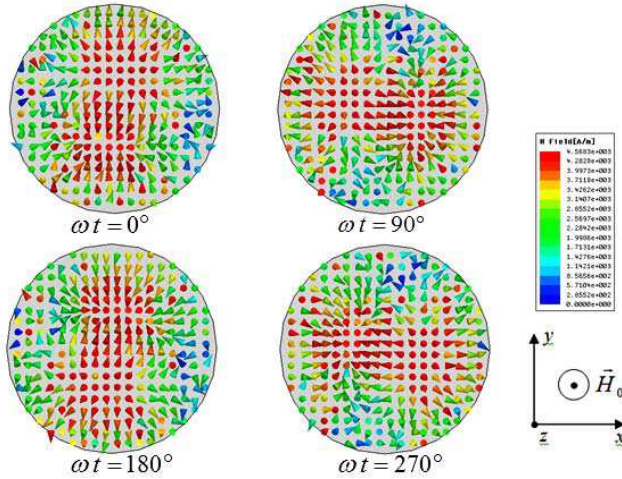


**Figure 8.** A top view for the numerically modeled magnetic field distributions on the upper plane of a ferrite disk for the for the 2nd resonance state ( $f = 8.66$  GHz) at different time phases. Figure reproduced from Ref. [46] @2009 IOP Publ. and Ref. [47] @2009 AIP.

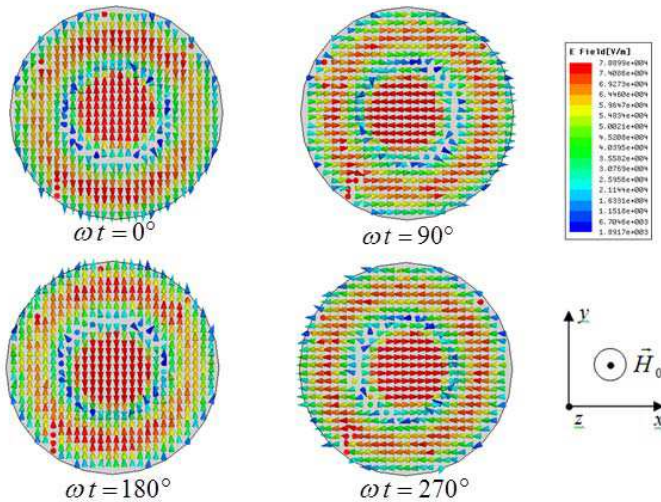


**Figure 9.** A top view for the numerically modeled electric field distributions on the upper plane of a ferrite disk for the for the 2nd resonance state ( $f = 8.66$  GHz) at different time phases. Figure reproduced from Ref. [46] @2009 IOP Publ. and Ref. [47] @2009 AIP.

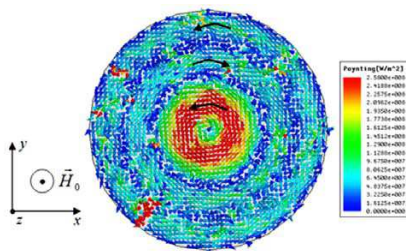


**Figure 10.** The power flow density distribution for the 2nd mode ( $f = 8.66$  GHz) in a quasi-2D ferrite disk. Figure reproduced from Ref. [46] ©2009 IOP Publ.

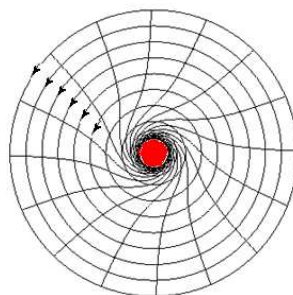


**Figure 11.** Schematic picture of the power-flow whirlpool in vacuum in the vicinity of a ferrite disk with MDM resonances.

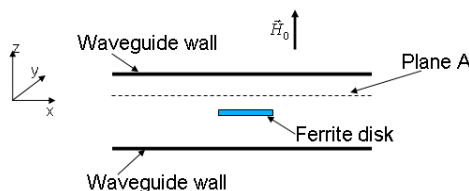


**Figure 12.**  $TE_{10}$ -mode rectangular waveguide with a normally magnetized ferrite disk. The  $xy$  vacuum plane (designated as plane A) inside a waveguide is situated at the distance of  $150 \mu\text{m}$  above an upper plane of a ferrite disk.

field. Schematically, this is illustrated in Figure 11.

Detailed studies of power-flow whirlpools in the near-field region of a MDM ferrite disk were made in Ref. [18]. In these studies, a ferrite disk was placed in a rectangular waveguide (see Figure 12). The spectrum was obtained at a constant bias field with variation of a signal frequency. Figure 13 shows the field confinement originated from the MDM vortices on a vacuum plane in a waveguide above a ferrite disk. No such a field confinement is observed at non-resonant frequencies. Because of symmetry breakings at MDM resonances, a ferrite disk strongly transforms the field structure of microwaves in an entire guiding system. Figure 14 shows the results obtained in Ref. [22]. As the time-phase changes, one observes strong transformations of the wavefront geometry. The wave front corresponds to a localized

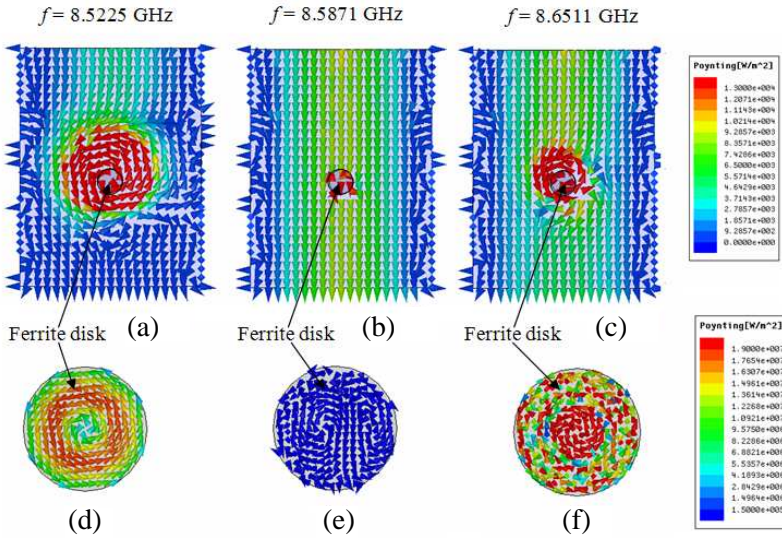


**Figure 13.** The field confinement originated from the MDM vortices in a ferrite disk. (a) The Poynting vector distributions for the fields on a vacuum plane (plane *A*) at the frequency ( $f = 8.5225$  GHz) of the 1st MDM resonance. (b) The same at the frequency ( $f = 8.5871$  GHz) between the MDM resonances. (c) The same at the frequency ( $f = 8.6511$  GHz) of the 2nd MDM resonance. (d) The Poynting vector distributions inside a ferrite disk at the frequency of the 1st resonance. (e) The same at the frequency between resonances. (f) The same at the frequency of the 2nd resonance. Figures reproduced from Ref. [18], ©2010 APS.

region where the electric field of a waveguide mode changes its sign. The inserts show enlarged pictures of the electric-field distributions immediately above a ferrite disk. It is very important to note that a geometrical structure of the shown fronts restores twice during a time period of the microwave radiation. For two next-coming fronts of incident waveguide-mode fields with the time-phase difference of  $\pi$ , one can see the same configuration of the wave fronts distorted due to scattering from a MDM particle. Very unique manipulation of microwave fields one observes in a case of interacting MDM particles [22]. Figure 15 shows the reflection coefficient of a waveguide with embedded coupled disks. The frequency region is related to the 1st MDM. It is worth noting that the frequency split in the resonance characteristics is extremely small. Its width is about 0.1%–0.2% of

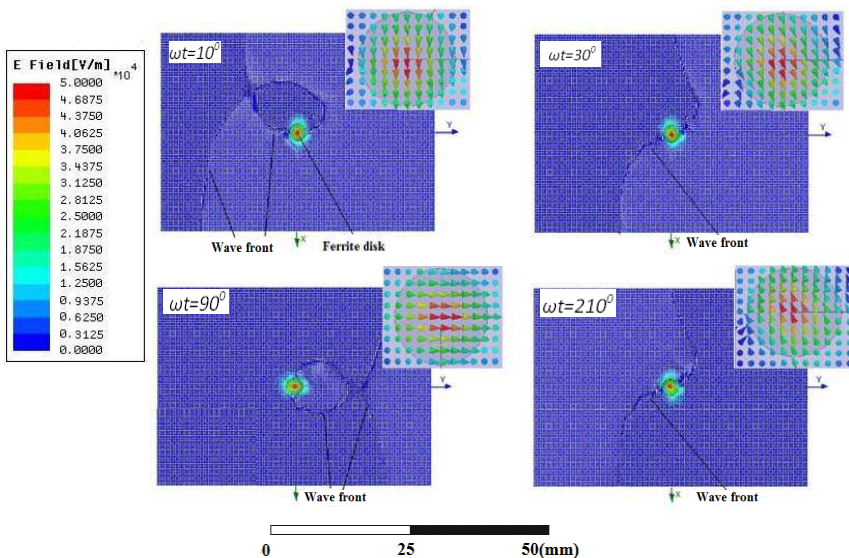


**Figure 14.** Transformations of the wave front of the electric field in a waveguide at the 1st resonance frequency on a vacuum above a ferrite disk at different time-phases. The inserts show enlarged pictures of the electric-field distributions immediately above a ferrite disk. Figure reproduced from Ref. [22], ©2012 IOP Publ.

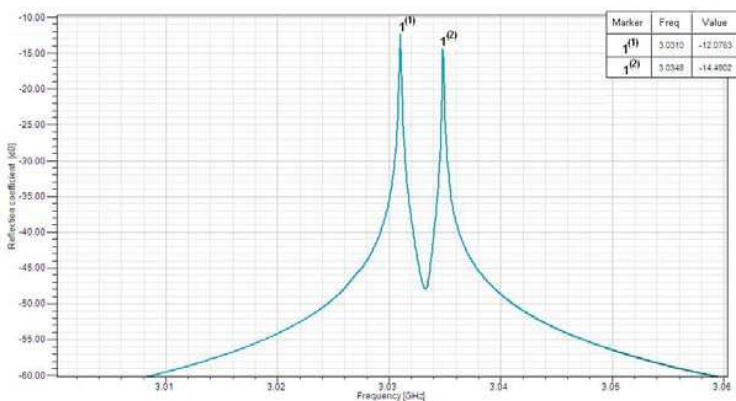


**Figure 15.** Reflection coefficient for two coupled disks at the frequency region of the 1st MDM. Figure reproduced from Ref. [22], ©2012 IOP Publ.

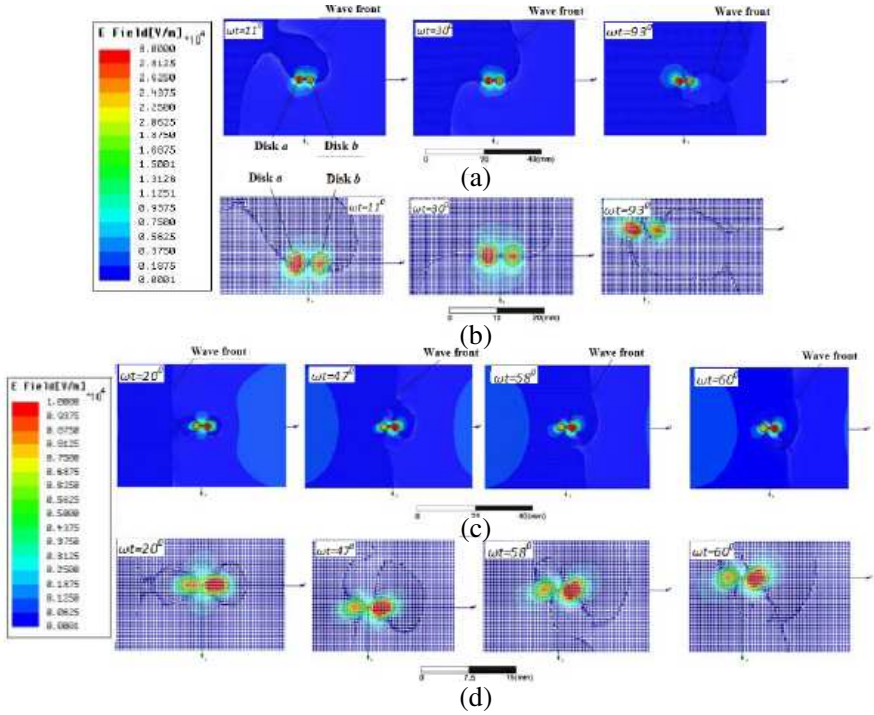


**Figure 16.** Positions of the wave fronts (localized regions where the electric field of a waveguide mode changes its sign) for coupled disks on a vacuum plane above ferrite disks. (a) At frequency of the 1st peak of the splitted resonance in a coupled-disk structure. (b) Enlarged pictures of the same distributions. (c) At frequency of the 2nd peak of the splitted resonance in a coupled-disk structure. (d) Enlarged pictures of the same distributions. Figures reproduced from Ref. [22], ©2012 IOP Publ.

frequency of an incident wave [22]. It was found also that the split-resonance response for coupled MDM particles is weakly dependent on distances between disks. One can observe almost the same response at short distances and at distances, which are very long in comparison with sizes of interacting particles. The shown characteristics could be important for development unique microwave filters. Figure 16 shows positions of the wave fronts of a waveguide mode for coupled MDM disks. There are two sets of pictures corresponding to even and odd modes of the coupled-disk structure.

In an array of MDM ferrite disks one can observe very peculiar behaviors of the near-field interactions [18]. The fact that every

disk acts as a structure with rotating fields and is characterized by a power-flow vortex, makes the problem solution non-trivial. Very unique properties of the MDM-vortex-particle arrays become apparent, when a structure has a center of symmetry. Figures 17 and 18 show,

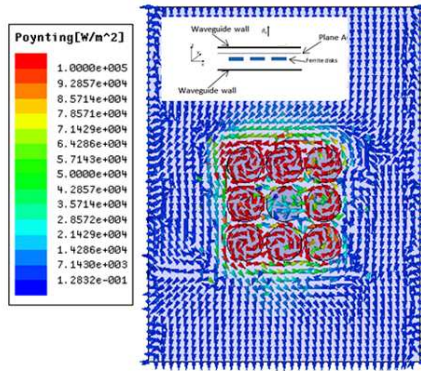


**Figure 17.** The power-flow-density distribution on a vacuum plane (plane A) for a structure of the in-plane nine-particle array with a center of symmetry. An insert shows a TE<sub>10</sub>-mode rectangular waveguide with a ferrite-disk array. Figure reproduced from Ref. [18], ©2010 APS.

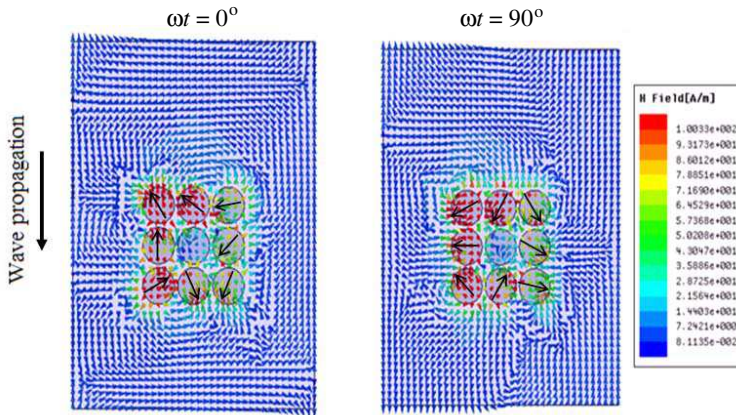


**Figure 18.** The magnetic-field picture on a vacuum plane (plane A) for a structure of a nine-particle array with a center of symmetry. Magnetic dipoles of the disks are shown conventionally by black arrows. Figure reproduced from Ref. [18], ©2010 APS.

respectively, the power-flow-density distribution and the magnetic-field picture for a structure of an in-plane nine-particle array with a center of symmetry. A peculiar property of a structure with a center of symmetry is a rotating wave running around the entire array. The power-flow-density distribution on a vacuum plane in a waveguide above a ferrite-disk array, shown in Figure 17, gives evidence for the Poynting-vector rotations in regions above every ferrite disk except the region above a central disk. There is also a resulting counterclockwise rotation of the Poynting vector around the entire array. For this array, the magnetic-field picture on the vacuum plane is the field of rotating magnetic dipoles. These magnetic dipoles are conventionally shown by black arrows in Figure 18. Every magnetic dipole has the counterclockwise rotation in time. For a certain phase of time, a circulation around the entire array shows a dynamics process in correlation with cyclic geometrical phase evolution of the disk-magnetic-dipole moments. For  $2\pi$  circulation, the magnetic-dipole vector accomplishes the  $2\pi$  geometric-phase rotation. It is worth noting that direction of the geometric-phase rotation is opposite to direction of circulation of an individual magnetic dipole. The results give evidence for a unique property of circulation of topological excitations around a center of symmetry of an array. A special attention should be paid for novel axial-symmetry metamaterial structures with rotational channeling of Skyrmion-like topological excitations. Unique symmetry properties of a system of interacting MDM ferrite disks allow make a proposition of a new-type subwavelength microwave metamaterial — the singular-microwaves metamaterials [17, 18].

Together with power-flow vortices, the near fields at the MDM resonances are characterized by the helicity properties. The near-field helicity parameters of a ferrite disk placed in a waveguide were

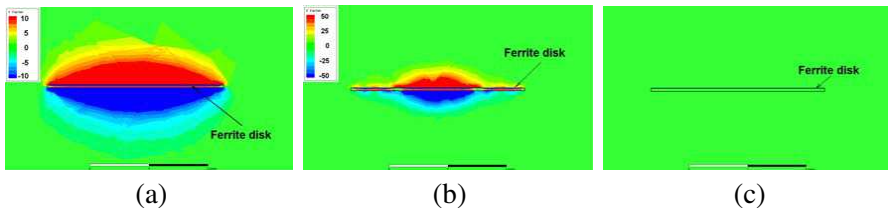


**Figure 19.** The near-field helicity parameters. (a) Near-field helicity at the resonance of the 1st MDM. (b) Near-field helicity at the resonance of the 2nd MDM. (c) Absence of the near-field helicity for non-resonant frequencies. Figures reproduced from Ref. [21], ©2013 APS and Ref. [50], ©2013 AIP.

calculated in Ref. [21] based on Equation (16). These results are shown in Figure 19. One can see distinctive properties of the near-field helicity at frequencies of the MDM resonances. At the same time, no helicity characteristics are observed at the non-resonant frequencies.

## 6. ENGINEERING OF NOVEL MICROWAVE FIELDS BY MDM FERRITE PARTICLES: THE NEAR- AND FAR-FIELD APPLICATIONS

Unique topological properties of the fields originated from MDM ferrite particles open perspective for novel microwave near- and far-field applications.

### 6.1. Novel Microwave Near-field Sensors for Material Characterization, Biology and Nanotechnology

Implementation of imaging in microwave frequencies gives the opportunity for electrodynamics experiments with natural materials and artificial structures. For subwavelength characterization of microwave material parameters, special metallic probes are mostly used. The near fields of such metallic probes are well known evanescent-mode fields [48, 49]. It becomes clear that new perfect lenses that can focus beyond the diffraction limit could revolutionize near-field microwave microscopy. In Ref. [50], a novel microwave near-field sensor with application to material characterization, biology, and nanotechnology has been proposed. This sensor is realized based on a small ferrite-disk resonator with MDM oscillations. The wavelength of the MDM oscillations in ferrite resonators is two-four orders of the magnitude less than the free-space electromagnetic-wave wavelength at the same microwave frequency [13]. Application of these properties in near-field microwave microscopy allows achieving submicron resolution much easier than in the existing microwave microscopes with standard resonant structures. Moreover, the near fields originated from a MDM ferrite disk have intrinsic chiral topology. It is sufficiently apparent that the problem of effective characterization of chemical and biological objects in microwaves can be solved when one develops special sensing devices with chiral probing fields. Another important aspect concerns spectral properties of MDM oscillations: a complete-set mode spectrum of MDM oscillations can be used to get a complete Fourier image (in the frequency or  $\vec{k}$ -space domain).

In Refs. [21, 43, 50] it was shown that dielectric samples loading a ferrite disk can cause strong transformations of the MDM spectra. These transformations are exhibited by two factors for an entire MDM

spectrum: (a) the frequency shift of the spectrum and (b) broadening of the spectrum. Moreover, due to dielectric loadings the Lorentzian-form resonant peaks of MDM oscillations can be transformed to the Fano-type resonances. The following consideration may explain, in particular, the frequency shift of the entire MDM spectrum. As we can see from Figures 6 and 9, an electric field inside a ferrite disk has both orbital and spin angular momentums. When an electrically polarized (due to the RF electric field of a microwave system) dielectric sample is placed above a ferrite disk, every separate dipole in a sample will precess around its own axis. For all the precessing electric dipoles, there is also an orbital phase running. Figure 20 represents a schematic picture of this effect. The mechanical torque exerted on a given electric dipole is defined as a cross product of the MDM electric field and the electric moment of the dipole. The torque exerting on the electric polarization due to the MDM electric field should be equal to reaction torque exerting on the magnetization in a ferrite disk. Because of this reaction torque, the precessing magnetic moment density of the

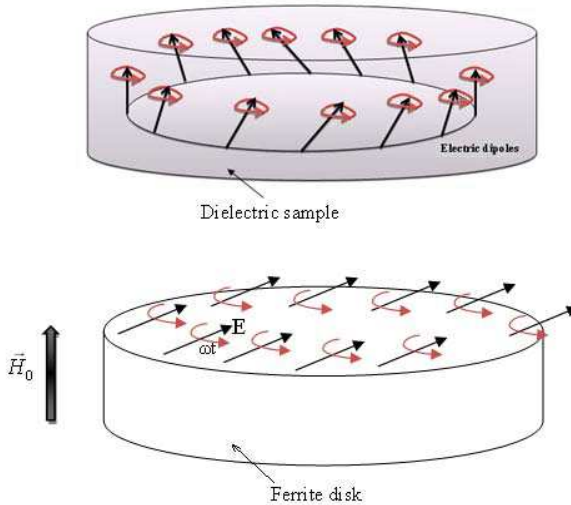


**Figure 20.** An electric field inside a ferrite disk has both orbital and spin angular momentums. When an electrically polarized dielectric sample is placed above a ferrite disk, electric dipoles in a dielectric sample precess and accomplish an orbital geometric-phase rotation. A bias magnetic field  $\vec{H}_0$  is directed normally to a disk plane. For an opposite direction of  $\vec{H}_0$ , one has an opposite rotation of an electric field and an opposite direction of precession of electric dipoles.

ferromagnet will be under additional mechanical rotation at a certain frequency  $\Omega$ . For the magnetic moment density of the ferromagnet,  $\vec{M}$ , the motion equation acquires the following form [2, 13]:

$$\frac{d\vec{M}}{dt} = -\gamma\vec{M} \times \left( \vec{H} - \frac{\Omega}{\gamma} \right), \tag{18}$$

The frequency  $\Omega$  is defined based on both, spin and orbital, momentums of the fields of MDM oscillations. One can see that at dielectric loadings, the magnetization motion in a ferrite disk is characterized by an effective magnetic field

$$\vec{H}_{eff} = \vec{H} - \frac{\Omega}{\gamma}. \tag{19}$$

So, the Larmor frequency of a ferrite structure with a dielectric loading should be lower than such a frequency in an unloaded ferrite disk. Figure 21 gives an example of transformation of the MDM spectrum due to dielectric loadings with different permittivity parameters. An insert shows a microwave microstrip structure (sensor) with a MDM ferrite disk and a sample under investigation [50]. In this figure, one can observe the shift of the MDM spectrum to lower frequencies.

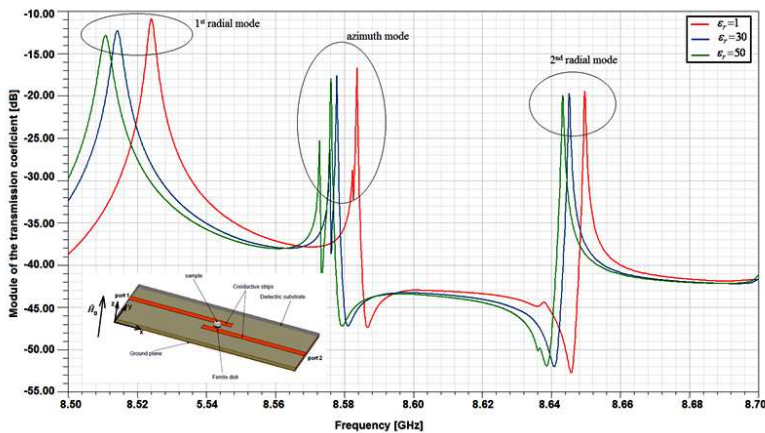


**Figure 21.** Transformation of the MDM spectrum due to dielectric loadings with different permittivity parameters. One observes the shift of the MDM spectrum to lower frequencies. An insert shows a microwave microstrip structure (sensor) with a MDM ferrite disk and a sample under investigation. Figure reproduced from Ref. [50], ©2013 AIP.

For effective localization of energy of MDM oscillations at micron and submicron near-field regions, special field concentrators should be used. In particular, there can be a thin metal wire placed on a surface of a ferrite disk [50]. Figure 22 shows a microstrip MDM sensor with a wire concentrator. A bias magnetic field  $\vec{H}_0$  is directed normally to a disk plane. In a shown structure, the helical waves localized in a ferrite disk are transmitted to the end of a wire electrode. The electric field of a microstrip structure causes a linear displacement of charge when interacting with a short piece of a wire, whereas the magnetic field of a MDM vortex causes a circulation of charge. Being combined, these two motions cause a helical motion of electrons, which includes translation and rotation. Due to such a behavior, one has a chiral surface electric

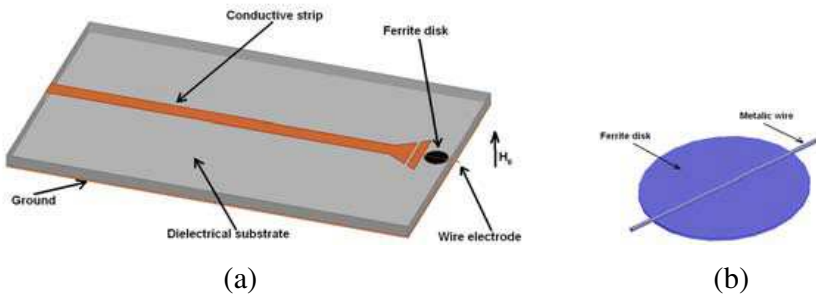


**Figure 22.** A sensor with a wire concentrator for localized material characterization. (a) Geometry of a microstrip structure. (b) A magnified picture of a MDM ferrite disk with a wire electrode. Figures reproduced from Ref. [50], ©2013 AIP.

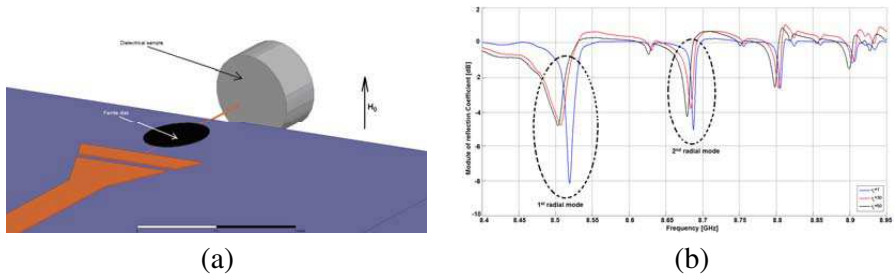


**Figure 23.** A microstrip structure for localized material characterization in a dielectric sample. (a) Geometry of a structure. (b) MDM spectra of the reflection coefficient at a dielectric loading. Figures reproduced from Ref. [50], ©2013 AIP.

current. The electric and magnetic fields at a butt end of a wire have mutually parallel components. All this results in appearing of the power-flow-density vortex and nonzero helicity density  $F$  at the butt end of a wire electrode. Figure 23 shows a microstrip structure with a field concentrator for localized material characterization and experimental results of the MDM spectra transformations for different dielectric samples.

Because of the near-field properties, a microstrip MDM sensor with a wire concentrator can be used for discrimination of enantiomeric structures at localized regions. When one changes oppositely an orientation of a bias magnetic field  $\vec{H}_0$ , one has an opposite rotation of the power flow and an opposite sign of the helicity density  $F$ . This allows localized sensing for prediction of samples with “right” and “left” handedness. Figure 24 shows the setup of the measurement system with a helical test structure for local determination of material

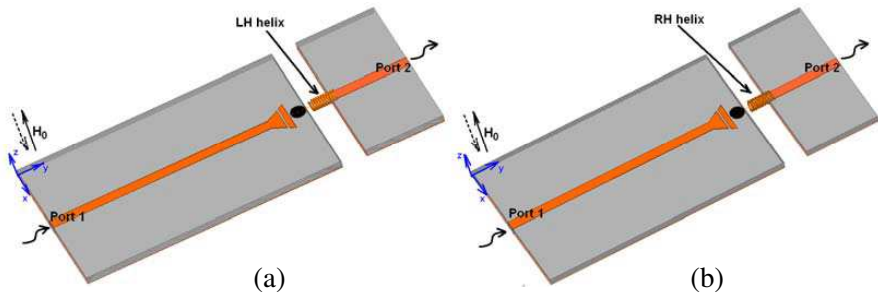


**Figure 24.** Sensor with small helix particles. (a) Left-handed helix particle. (b) Right-handed helix particle. Figures reproduced from Ref. [50], ©2013 AIP.

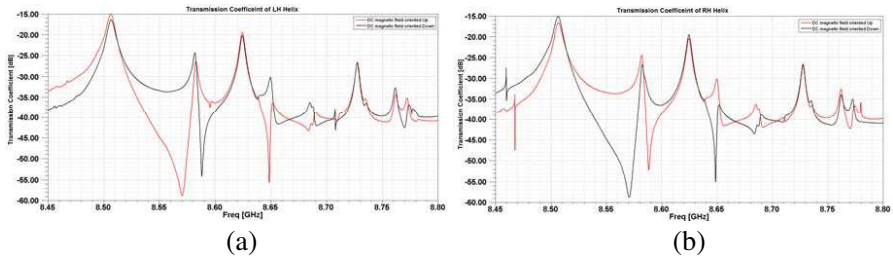


**Figure 25.** Transmission coefficients for small helix particles. (a) Left-handed helix particle. (b) Right-handed helix particle. Figures reproduced from Ref. [50], ©2013 AIP.

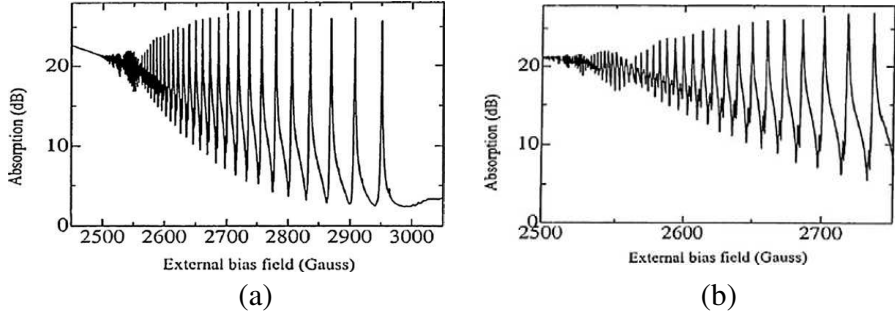


**Figure 26.** (a) Fano-resonant spectrum obtained in a ridged-waveguide microwave structure with an embedded MDM ferrite disk. (b) An enlarged picture of the high-order-peak part of the same spectrum. Figures (a) and (b) reproduced from Ref. [41], ©2004 Elsevier Publ.

chirality [50]. As a localized test structures mimicking objects with chiral properties, small metallic helices were used. A wire concentrator is placed near a metallic helix without an electric contact with it. In Figure 25, one can see numerical results of the transmission coefficients for the left-handed and right-handed helical test structure, respectively. The spectral characteristics are obtained for two opposite orientations of a bias magnetic field  $\vec{H}_0$ . The results in Figure 25 exhibit very specific symmetry properties: one observes restoration of an entire transmission spectrum when handedness of a sample is changed together with change of direction of a bias magnetic field.

## 6.2. Fano-resonant Interference. Generating Far-field Angular Momenta from Near-field Microwave Chirality

Nowadays, in optics, we are witnesses of intensive development of new capabilities of interaction of phase-structured far- and near-field electromagnetic radiations. Also, interaction of phase-structured light with matter is a new branch of optics. These studies concern, in particular, phase analyses of near-field images in subwavelength optical microscopy [51], Fano-resonant interference for effective biosensing [52], interaction of far-field optical radiation with plasmonic structures characterizing by near-field chirality [8,9], generation of far-field angular momenta from near-field optical chirality [10], generation of twisted light (or light beams carrying orbital angular momentum) [53], etc.. In microwaves, such capabilities of interaction of phase-structured far- and near-field radiations have not been studied sufficiently.

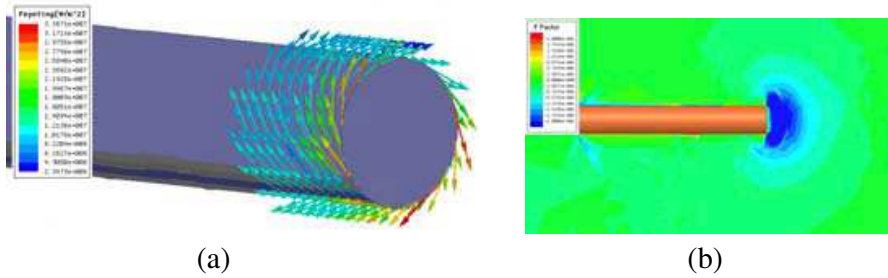


**Figure 27.** Field structure on a butt end of a wire concentrator: (a) the power-flow-density vortex and (b) the helicity density  $F$ . When one changes oppositely an orientation of a bias magnetic field  $\vec{H}_0$ , one has an opposite rotation of the power flow and an opposite sign of the helicity density  $F$  (red colored instead of blue colored). Figures (a) and (b) reproduced from Ref. [50], ©2013 AIP.

Since the fields originated from a MDM ferrite particle are distinguished by strong topological phase variations, new capabilities for application of phase-structured microwave radiation become evident. Long radiative lifetimes of MDMs combine strong subwavelength confinement of electromagnetic energy with a narrow spectral line width and may carry the signature of Fano resonances. Figures 21 and 25 in this paper give an example of the Fano-resonant spectra. In some microwave structures, interaction of the MDM ferrite particle with its environment may have a more pronounced effect of the Fano-resonance interference [23, 41–43]. Figure 26 shows an example of such profound Fano-resonant oscillations obtained in a ridged-waveguide microwave structure [41]. It is worth noting that there is a strong analogy of this spectrum with the Fano interference observed in semiconductor quantum dots [54]. Precise quantitative phase measurements carried out based on such an interference effect, can change microwave imaging science in fundamental ways. Together with fundamental properties of this interaction, distinguishing by the time and space symmetry breakings, novel applications are very attractive. The observed microwave Fano resonances exhibit very strong sensitivity to changes of the local environment. Perhaps the most straightforward application of Fano resonances in MDM structures may concern the development of microwave sensors for chemical and biological objects with chiral properties [21, 50].

Another subject of a great interest in microwaves can be generating far-field orbital angular momenta from near-field chirality of MDM structures. On a butt end of a wire concentrator, shown

in Figure 22, one has the power-flow-density vortex and the non-zero helicity density. Figure 27 shows the field structure on a butt end of this electrode. When one changes oppositely an orientation of a bias magnetic field  $\vec{H}_0$ , one has an opposite rotation of the power flow and an opposite sign of the helicity density  $F$ . Being used in Ref. [50] as a near-field sensor, this device can also be used as a small antenna for generation and applications of twisted microwave radiation. The interaction of such twisted microwave radiation with material structures will appear as a promising field of research and technology. This also opens perspective for novel communication microwave systems with topological-phase modulation.

## 7. CONCLUSION

Microwave ferrite structures with a reduced dimensionality brings into play new effects, which should be described based on the quantized picture and demonstrate the properties of artificial atomic structures. The subwavelength confinement of the electromagnetic fields due to ferrite particles with MDM oscillations is related to the field quantization and symmetry breakings. A distinctive feature of the near fields originated from MDM ferrite particles — the ME fields — is the presence of the helicity structure.

Use of subwavelength MDM fields with energy localization and symmetry breakings opens a perspective for novel near- and far-field microwave applications. Unique topological properties of these fields can be used to study specific structural effects in natural and artificial materials. Presently, direct detection of biological structures in microwave frequencies and understanding of the molecular mechanisms of nonthermal microwave effects is a problem of a great importance. The problem of effective characterization of chemical and biological objects in microwaves can be solved when one develops special sensing devices with microwave chiral probing fields. We showed that small ferrite-disk resonators with magnetic-dipolar-mode (MDM) oscillations may create microwave superchiral fields with strong subwavelength localization of electromagnetic energy. Based on such properties of the fields, we propose a novel near-field microwave sensor with application to material characterization, biology, and nanotechnology.

Generation of far-field orbital angular momenta from near-field chirality of MDM structures is another subject of a great interest in microwaves. This will allow creation of localized microwave radiation with spin and orbital angular momentums. Such propagating twisted microwave fields can be used for material studies and communication systems with topological-phase modulation.

## REFERENCES

1. Jackson, J. D., *Classical Electrodynamics*, 2nd Edition, Wiley, New York, 1975.
2. Landau, L. D. and E. M. Lifshitz, *Electrodynamics of Continuous Media*, 2nd Edition, Pergamon, Oxford, 1984.
3. Barnes, W. L., A. Dereux, and T. W. Ebbesen, "Surface plasmon subwavelength optics," *Nature*, Vol. 424, 824–830, 2003.
4. Lee, B., I.-M. Lee, S. Kim, D.-H. Oh, and L. Hesselink, "Review on subwavelength confinement of light with plasmonics," *J. Mod. Opt.*, Vol. 57, No. 16, 1479–1497, 2010.
5. Ahn, W., S. V. Boriskina, Y. Hong, and B. M. Reinhard, "Electromagnetic field enhancement and spectrum shaping through plasmonically integrated optical vortices," *Nano Lett.*, Vol. 12, 219–227, 2012.
6. Rütting, F., A. I. Fernández-Domínguez, L. Martín-Moreno, and F. J. García-Vidal, "Subwavelength chiral surface plasmons that carry tuneable orbital angular momentum," *Phys. Rev. B*, Vol. 86, 075437, 2012.
7. Tang, Y. and A. E. Cohen, "Optical chirality and its interaction with matter," *Phys. Rev. Lett.*, Vol. 104, 163901, 2010.
8. Hendry, E., T. Carpy, J. Johnston, M. Popland, R. V. Mikhaylovskiy, A. J. Laphorn, S. M. Kelly, L. D. Barron, N. Gadegaard, and M. Kadodwala, "Ultrasensitive detection and characterization of biomolecules using superchiral fields," *Nat. Nanotechnol.*, Vol. 5, 783–787, 2010.
9. Hentschel, M., M. Schäferling, T. Weiss, N. Liu, and H. Giessen, "Three-dimensional chiral plasmonic oligomers," *Nano Lett.*, Vol. 12, 2542–2547, 2012.
10. Gorodetski, Y., A. Drezet, C. Genet, and T. W. Ebbesen, "Generating far-field orbital angular momenta from near-field optical chirality," *Phys. Rev. Lett.*, Vol. 110, 203906, arXiv:1302.0678, 2013.
11. Miroshnichenko, A. E., S. Plach, and Y. S. Kivshar, "Fano resonances in nanoscale structures," *Rev. Mod. Phys.*, Vol. 82, 2257–2298, 2010.
12. Luk'yanchuk, B., N. I. Zheludev, S. A. Maier, N. J. Halas, P. Nordlander, H. Giessen, and C. T. Chong, "The Fano resonance in plasmonic nanostructures and metamaterials," *Nature Mater.*, Vol. 9, 707–715, 2010.

13. Gurevich, A. and G. Melkov, *Magnetic Oscillations and Waves*, CRC Press, New York, 1996.
14. Kamenetskii, E. O., “Energy eigenstates of magnetostatic waves and oscillations,” *Phys. Rev. E*, Vol. 63, 066612, 2001.
15. Kamenetskii, E. O., M. Sigalov, and R. Shavit, “Quantum confinement of magnetic-dipolar oscillations in ferrite discs,” *J. Phys.: Condens. Matter*, Vol. 17, 2211–2231, 2005.
16. Kamenetskii, E. O., “Vortices and chirality of magnetostatic modes in quasi-2D ferrite disc particles,” *J. Phys. A: Math. Theor.*, Vol. 40, 6539–6559, 2007.
17. Kamenetskii, E. O., “Helical-mode magnetostatic resonances in small ferrite particles and singular metamaterials,” *J. Phys.: Condens. Matter*, Vol. 22, 486005, 2010.
18. Kamenetskii, E. O., M. Sigalov, and R. Shavit, “Manipulating microwaves with magnetic-dipolar-mode vortices,” *Phys. Rev. A*, Vol. 81, 053823, 2010.
19. Kamenetskii, E. O., R. Joffe, and R. Shavit, “Coupled states of electromagnetic fields with magnetic-dipolar-mode vortices: MDM-vortex polaritons,” *Phys. Rev. A*, Vol. 84, 023836, 2011.
20. Kamenetskii, E. O., “Microwave magnetoelectric fields,” arXiv:1111.4359, 2011.
21. Kamenetskii, E. O., R. Joffe, and R. Shavit, “Microwave magnetoelectric fields and their role in the matter-field interaction,” *Phys. Rev. E*, Vol. 87, 023201, 2013.
22. Berezin, M., E. O. Kamenetskii, and R. Shavit, “Topological-phase effects and path-dependent interference in microwave structures with magnetic-dipolar-mode ferrite particles,” *J. Opt.*, Vol. 14, 125602, 2012.
23. Kamenetskii, E. O., G. Vaisman, and R. Shavit, “Fano resonances of microwave structures with embedded magneto-dipolar quantum dots,” arXiv:1309.2792, 2013.
24. McDonald, K. T., “An electrostatic wave,” arXiv:physics/03120-25, 2003.
25. McDonald, K. T., “Magnetostatic spin waves,” arXiv:physics/03-12026, 2003.
26. Søndergaard, T. and S. Bozhevolnyi, “Slow-plasmon resonant nanostructures: Scattering and field enhancements,” *Phys. Rev. B*, Vol. 75, 073402, 2007.
27. Pelton, M., J. Aizpurua, and G. Bryant, “Metal-nanoparticle plasmonics,” *Laser & Photon. Rev.*, Vol. 2, 136–159, 2008.

28. Stockman, M. I., S. V. Faleev, and D. J. Bergman, "Localization versus delocalization of surface plasmons in nanosystems: Can one state have both characteristics?," *Phys. Rev. Lett.*, Vol. 87, 167401, 2001.
29. Li, K., M. I. Stockman, and D. J. Bergman, "Self-similar chain of metal nanospheres as an efficient nanolens," *Phys. Rev. Lett.*, Vol. 91, 227402, 2003.
30. Bergman, D. J. and D. Stroud, "Theory of resonances in the electromagnetic scattering by macroscopic bodies," *Phys. Rev. B*, Vol. 22, 3527–3539, 1980.
31. Mayergoyz, I. D., D. R. Fredkin, and Z. Zhang, "Electrostatic (plasmon) resonances in nanoparticles," *Phys. Rev. B*, Vol. 72, 155412, 2005.
32. Brongersma, M. L., J. W. Hartman, and H. A. Atwater, "Electromagnetic energy transfer and switching in nanoparticle chain arrays below the diffraction limit," *Phys. Rev. B*, Vol. 62, R16356–R16359, 2000.
33. Maier, S. M., P. G. Kik, and H. A. Atwater, "Optical pulse propagation in metal nanoparticle chain waveguides," *Phys. Rev. B*, Vol. 67, 205402, 2003.
34. Davis, T. J., K. C. Vernon, and D. E. Gómez, "Effect of retardation on localized surface plasmon resonances in a metallic nanorod," *Opt. Express*, Vol. 17, 23655–23663, 2009.
35. Wang, Z. B., B. S. Luk'yanchuk, M. H. Hong, Y. Lin, and T. C. Chong, "Energy flow around a small particle investigated by classical Mie theory," *Phys. Rev. B*, Vol. 70, 035418, 2004.
36. Bashevoy, M. V., V. A. Fedotov, and N. I. Zheludev, "Optical whirlpool on an absorbing metallic nanoparticle," *Opt. Express*, Vol. 13, 8372–8379, 2005.
37. Tribelsky, M. I. and B. S. Luk'yanchuk, "Anomalous light scattering by small particles," *Phys. Rev. Lett.*, Vol. 97, 263902, 2006.
38. Walker, L. R., "Magnetostatic modes in ferromagnetic resonance," *Phys. Rev.*, Vol. 105, 390–399, 1957.
39. Dillon, Jr., J. F., "Magnetostatic modes in disks and rods," *J. Appl. Phys.*, Vol. 31, 1605–1614, 1960.
40. Yukawa, T. and K. Abe, "FMR spectrum of magnetostatic waves in a normally magnetized YIG disk," *J. Appl. Phys.*, Vol. 45, 3146–3153, 1974.
41. Kamenetskii, E. O., A. K. Saha, and I. Awai, "Interaction of magnetic-dipolar modes with microwave-cavity electromagnetic

- fields,” *Phys. Lett. A*, Vol. 332, 303–309, 2004.
42. Sigalov, M., E. O. Kamenetskii, and R. Shavit, “Eigen electric moments and magnetic-dipolar vortices in quasi-2D ferrite disks,” *Appl. Phys. B*, Vol. 93, 339–343, 2008.
  43. Sigalov, M., E. O. Kamenetskii, and R. Shavit, “Electric self-inductance of quasi-two-dimensional magnetic-dipolar-mode ferrite disks,” *J. Appl. Phys.*, Vol. 104, 053901, 2008.
  44. Kamenetskii, E. O., R. Shavit, and M. Sigalov, “Quantum wells based on magnetic-dipolar-mode oscillations in disk ferromagnetic particles,” *Europhys. Lett.*, Vol. 64, 730–736, 2003.
  45. Pozar, D. M., *Microwave Engineering*, 3rd Edition, Wiley, New York, 2004.
  46. Sigalov, M., E. O. Kamenetskii, and R. Shavit, “Magnetic-dipolar and electromagnetic vortices in quasi-2D ferrite disks,” *J. Phys.: Condens. Matter*, Vol. 21, 016003, 2009.
  47. Kamenetskii, E. O., M. Sigalov, and R. Shavit, “Tellegen particles and magnetoelectric metamaterials,” *J. Appl. Phys.*, Vol. 105, 013537, 2009.
  48. Anlage, S. M., D. E. Steinhauer, B. J. Feenstra, C. P. Vlahacos, and F. C. Wellstood, “Near-field microwave microscopy of material properties,” arXiv: cond-mat/0001075, 2000.
  49. Rosner, B. T. and D. W. van der Weide, “High-frequency near-field microscopy,” *Rev. Sci. Instrum.*, Vol. 73, 2505–2525, 2002.
  50. Joffe, R., E. O. Kamenetskii, and R. Shavit, “Novel microwave near-field sensors for material characterization, biology and nanotechnology,” *J. Appl. Phys.*, Vol. 113, 063912, 2013.
  51. Carney, P. S., B. Deutch, A. A. Govyadinov, and R. Hillenbrand, “Phase in nanooptics,” *ACS NANO*, Vol. 6, 8–12, 2012.
  52. Wu, C., A. B. Khanikaev, R. Adato, N. Arju, A. Ali Yanik, H. Altug, and G. Shvets, “Fano-resonant asymmetric metamaterials for ultrasensitive spectroscopy and identification of molecular monolayers,” *Nature Mater.*, Vol. 11, 69–75, 2012.
  53. Andrews, D. L., *Structured Light and Its Applications: An Introduction to Phase-structured Beams and Nanoscale Optical Forces*, Academic Press, 2008.
  54. Johnson, C., C. M. Marcus, M. P. Hanson, and A. C. Gossard, “Coulomb-modified Fano resonance in a one-lead quantum dot,” *Phys. Rev. Lett.*, Vol. 93, 106803, 2004.